International Journal of Robotics and Control Systems
Vol. 5, No. 1, 2025, pp. 640-660
ISSN 2775-2658
http://pubs2.ascee.org/index.php/ijrcs

A Comparative Study of PID, FOPID, ISF, SMC, and FLC Controllers for DC Motor Speed Control with Particle Swarm Optimization

Muhammad Haryo Setiawan [a,1], Alfian Ma'arif [a,2,*], Much. Fuad Saifuddin [b,3], Wael A. Salah [c,4]

[a] Electrical Engineering Department, Universitas Ahmad Dahlan, Jl. South Ring Road, Yogyakarta, 55191, Indonesia
[b] Association for Scientific Computing Electronics and Engineering (ASCEE)
[c] Palestine Technical University – Kadoorie, Tulkarm, Palestine
[1] haryo.setiawan09@gmail.com; [2] alfian.ma'arif@ee.uad.ac.id; [3] mfuad@ascee.org; [4] wael.salah@ptuk.edu.ps
* Corresponding Author

ARTICLE INFO

Article history
Received December 08, 2024
Revised January 23, 2025
Accepted February 03, 2025

Keywords
DC Motor;
PID Control;
FOPID Control;
Integral State Feedback;
Sliding Mode Control;
Fuzzy Logic Control;
Particle Swarm Optimization

ABSTRACT

Direct Current (DC) motors are extensively used in various applications due to their versatile and precise control capabilities. However, they face operational challenges such as speed instability and sensitivity to load variations and external disturbances. This study compares the performance of several advanced control methods—Proportional Integral Derivative (PID), Fractional Order PID (FOPID), Integral State Feedback (ISF), Sliding Mode Control (SMC), and Fuzzy Logic Controller (FLC) for DC motor control. Particle Swarm Optimization (PSO) is employed to optimize the tuning parameters of PID, FOPID, ISF, and SMC controllers, while FLC is implemented without optimization. The simulation results indicate that the PSO-FOPID controller exhibits the best overall performance, characterized by the fastest rise and settling times and the lowest ITSE, despite a minor overshoot. The PSO-PID controller also performs well, with fast response times, although it is less efficient in terms of settling time and ITSE compared to PSO-FOPID. The OBL/HGSO-PID controller, while stable and overshoot-free, has a slower response. The PSO-ISF controller shows the highest stability with the lowest SSE values, making it suitable for applications requiring high stability. The PSO-SMC controller demonstrates good stability but is slightly slower than PSO-ISF. The FLC controller, however, performs the worst, with significant overshoot and long recovery times, making it unsuitable for fast and precise control applications. The robustness analysis under varying motor parameters further confirms the superiority of the PSO-FOPID controller, which outperforms OBL/HGSO and OBL-MRFO-SA optimizations across both PID and FOPID controllers, making it the most effective solution for applications requiring high precision and rapid response.

1. Introduction

Direct Current (DC) motors are widely used across various fields due to their versatility and ease of control. Their ability to provide a broad range of speeds makes them ideal for applications in both household and industrial [1], [2]. Household devices such as air conditioner [3], fans [4], washing machines [5], vacuum cleaners [6], automatic floor cleaner [7], and water pumps [8]. In livestock

farming sector used for automatically feeding system [9], [10]. Furthermore, in the medical field, DC motors play an important role in devices such as infusion pumps [11], [12], electric wheelchairs [13], ventilators [14], and bed adjusters that can improve the patient's comfort and safety [15]. Security applications, including electric door locks [16], and automated gates [17], also depend on the reliability of DC motors. In energy sector, used for tracking, such as solar tracker for photovoltaic [18], [19].

In industrial environments, DC motors are integral to the functioning of machines like belt conveyors [20], [21], robotic systems (such as arm robot [7], [22], [23], grippers, mobile robots [24]-[26], and balancing systems [27], [28]), and unmanned aerial vehicles (UAVs) [29], [30]. In the transportation sector, electric motorcycles [31], electric cars [32], and even electric buses [33]. Their precise control and efficient performance are crucial in applications that require stability and adaptability, particularly when handling varying loads and speeds [34], [35]. The flexibility of DC motors makes them a key component in technologies ranging from everyday household items to sophisticated industrial equipment, underscoring their significance in diverse sectors [36].

However, despite their many advantages, DC motors face operational challenges, particularly with speed instability caused by load variations, changes in system parameters, and external disturbances [37], [38]. These factors can compromise motor performance, making it difficult to maintain consistent speed and efficiency [39]. To address these challenges, advanced control methods are necessary to ensure the motor operates optimally under dynamic conditions [40]. The ability to regulate motor speed effectively is crucial to maintaining system stability [41] and achieving desired performance levels, especially in applications that require precision [42], [43].

To address these challenges, various control methods have been developed, including PID [44], Fractional Order PID (FOPID) [45], Integral State Feedback (ISF) [46], Sliding Mode Controller (SMC) [47], and Fuzzy Logic Controller (FLC) [48]. PID is widely used for its simplicity and effectiveness [49], while FOPID offers greater adaptability robustness and nonlinearity by incorporating fractional calculus [50]. ISF enhances system stability and robustness [51], SMC provides high accuracy under nonlinear conditions [52], and FLC excels in handling uncertainties and complex dynamics without requiring an accurate mathematical model [53].

While these advanced control strategies exhibit significant advantages, tuning their parameters manually is a time-consuming process, especially in systems with complex dynamics [54]. Optimization methods, such as Particle Swarm Optimization (PSO), have been widely adopted to streamline this process [55], [56]. Other optimization techniques, such as Genetic Algorithms (GA) [57], Differential Evolution (DE) [58], Ant Colony Optimization (ACO) [59], and Grey Wolf Optimization (GWO) [60] have also been employed to address similar challenges. These methods are designed to enhance the precision and efficiency of parameter tuning, enabling the deployment of optimized controllers that achieve superior performance with minimal effort. By leveraging these optimization algorithms, engineers can ensure that control strategies such as PID, FOPID, ISFC, and SMC operate at their full potential, meeting the demanding requirements of modern DC motor applications.

Previous research on DC motor control using PID controllers was conducted by Ekinci, S., et al. [44], where they implemented a conventional PID control approach tuned using the Opposition-Based Henry Gas Solubility Optimization (OBL/HGSO) algorithm. In their research, they reported achieving a rise time of 0.052278 seconds, a settling time of 0.0917148 seconds, and an overshoot of 0%, indicating a fast and stable response without any overshoot. The use of OBL/HGSO for PID tuning enhanced the controller's ability to achieve these desirable transient characteristics. Despite the promising results, the inherent limitations of conventional PID control in handling nonlinearity and improving performance under varying conditions remain a challenge.

Other previous research on DC motor control using FOPID controllers was conducted by Ekinci, S., et. al. [45], where they implemented FOPID controller tuned using the Opposition-Based Hybrid Manta Ray Foraging Optimization and Simulated Annealing Algorithm (OBL-MRFO-SA). The

results reported by the researchers showed that a rise time of 0.0214 seconds, a settling time of 0.0339 seconds and an overshoot of 0% were achieved. These results indicate a rapid response without overshoot in comparison to the conventional PID Controller [44]. The use of OBL-MRFO-SA for FOPID tuning enhanced the controller's ability to achieve these desirable transient characteristics.

In this study, the primary objective is to compare the performance of various controllers, including PID, FOPID, ISF, SMC, and FLC, for DC motor control. While PSO is utilized to optimize the tuning parameters of PID, FOPID, ISF, and SMC controllers, the FLC is implemented without PSO-based tuning. This comprehensive comparison aims to evaluate the strengths and limitations of each controller under dynamic operating conditions, highlighting their effectiveness in addressing challenges such as speed instability, load variations, and external disturbances. The insights gained from this research will contribute to identifying the most suitable control strategy for enhancing the performance and stability of DC motor systems.

2. Method

2.1. DC Motor System Model

The speed of the DC motor was regulated through armature voltage control, with the closed-loop system depicted in Fig. 1. The motor's actual speed (ω) and the reference speed (ω_{ref}) were used as feedback parameters. The system's electrical and mechanical properties are summarized in Table 1, which includes details of armature resistance, inductance, motor inertia, friction constant, and electromotive force constant.

Table 1. DC motor electrical and mechanical parameters

Parameter	Description	Value	Unit
R_a	Armature resistance	0.4	Ω
L_a	Armature inductance	2.7	H
J	Motor inertia	0.0004	$kg.m^2$
B	Motor friction constant	0.0022	$N.m.s/rad$
K_m	Motor torque constant	0.015	$N.m/A$
K_b	Electromotive force constant	0.05	$V.s$

Open loop transfer function of DC motor is obtained as follows. The induced voltage $e_b(t)$ for a constant flux is proportional to the angular velocity $\omega(t) = \frac{d\theta}{dt}$ and given in (1).

$$e_b(t) = K_b \frac{di_a(t)}{dt} = K_b \omega(t) \tag{1}$$

The armature voltage $e_a(t)$ is used to govern the speed of an armature-controlled DC motor. The armature circuit's differential equation is given in (2).

$$e_a(t) = L_a \frac{di_a(t)}{dt} + R_a i_a(t) + e_b(t) \tag{2}$$

Assuming the load torque is zero, a corresponding torque (sum of inertia and friction torques) is produced by the armature current as provided in (3).

$$T(t) = J \frac{d\omega(t)}{dt} + B\omega(t) = K_m i_a(t) \tag{3}$$

The Laplace transforms of (1) to (3) with zero initial conditions are given as follows:

$$E_b(s) = K_b \Omega \tag{4}$$

$$E_a(s) = (L_a + R_a)I_a(s) + E_b(s) \tag{5}$$

$$T(s) = (Js + B)\Omega(s) = \mathrm{K_m} I_a(s) \tag{6}$$

Hence, the open loop transfer function describing the relationship between input voltage and the output speed of DC motor can be written in (7).

$$\frac{\Omega(s)}{E_a(s)} = \frac{K_m}{(L_a R_a)(Js + B) + K_b K_m}, for\ T_{load} = 0 \tag{7}$$

Furthermore, the relationship between motor speed (ω) and load torque (T_{load}) when the input voltage (E_a) is zero can also be given by the following transfer function in (8).

$$\frac{\Omega(s)}{T_{load}(s)} = \frac{(L_a s + R_a)}{(L_a s + R_a)(Js + B) + K_b K_m}, for\ E_a = 0 \tag{8}$$

Substituting DC motor parameter values in (7) dan (8), the following open loop transfer function is obtained as.

$$G_{open-loop}(s) = \begin{cases} \dfrac{\Omega(s)}{E_a(s)} = \dfrac{15}{1.08s^2 + 6.1s + 1.63}, for\ T_{load} = 0 \\ \dfrac{\Omega(s)}{\mathrm{T_{load}}(s)} = -\dfrac{(2700 + 400)}{1.08s^2 + 6.1s + 1.63}, for\ E_a = 0 \end{cases} \tag{9}$$

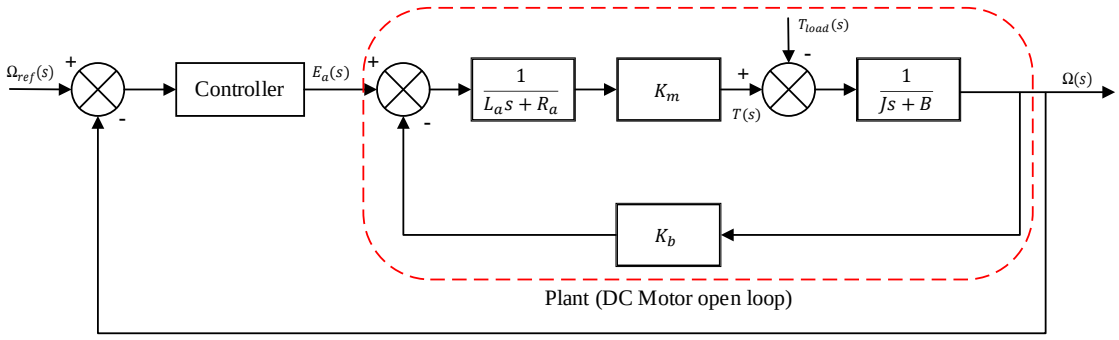

Fig. 1. Closed loop DC motor system

2.2. Proportional Integral Derivative (PID) Controller

PID controllers are one of the most widely used methods in control systems for regulating and stabilizing dynamic systems [61], [62]. They operate based on feedback control, where the control signal is generated from the error $(e(t))$ between the reference input and the actual output $(u(t))$ [63]. The general equation for a PID controller in the Laplace domain is given by:

$$PID(s) = K_p + \frac{K_i}{s} + K_d s \tag{10}$$

The proportional term (K_p) generates a control action proportional to the current error, which improves the system's response time but cannot eliminate steady-state error. The integral term (K_i) sums the accumulated past errors to remove steady-state error, ensuring the output matches the reference input. However, excessive integral action may cause overshoot and instability. The derivative term (K_d) predicts future errors by responding to the rate of change of the error, improving stability and reducing overshoot, though it is sensitive to noise in the error signal [64]-[66].

PID controllers are known for their simplicity and effectiveness in managing system dynamics. Their wide applicability ranges from motor speed control regulation to process automation and

robotics. They provide a balance between responsiveness, accuracy, and stability. However, they may struggle in systems with significant time delays or strong nonlinearities.

2.3. Fractional Order PID (FOPID) Controller

FOPID controllers offer a promising approach for improving the performance of DC motors [67]. In contrast to conventional PID controllers, which are founded upon integer-order derivatives [68], [69], FOPID controllers employ fractional-order terms to facilitate more adaptable control and can accommodate nonlinear systems [70], [71]. The general equation of FOPID Controller is given by:

$$FOPID(s) = K_p + K_i \frac{1}{s^{\lambda}} + K_d s^{\mu} \tag{11}$$

The main advantage of FOPID controllers is their ability to adjust the proportional, integral, and derivative terms using fractional order parameters λ and μ, providing greater flexibility and the ability to handle stable nonlinear systems [72]-[75], The fractional orders λ and μ allow for finer control, which helps to reduce steady-state error, decrease overshoot, and improve robustness to external disturbances or varying system parameters [76], [77].

The FOPID controller retains structural similarities with the conventional PID controller but with broader adaptability due to the fractional-order terms. This makes FOPID particularly effective in systems with complex dynamics and nonlinear disturbances, which are challenging to control using standard PID controllers.

2.4. Integral State Feedback (ISF) Controller

The ISF Controller provides an effective mechanism for managing system performance by integrating feedback from all state variables, enabling improved system stability and robustness against disturbances [78]. This approach excels in addressing system-wide dynamics and ensuring steady-state accuracy, making it well-suited for DC motor control. ISF Controller ability to handle dynamic variations and disturbances enhances its reliability and application in high-precision motor control systems [79]. Its integration of state variables contributes to a more cohesive control structure, particularly in systems that demand resilience to fluctuating loads or environmental changes [80]. The equation of ISF can be written as:

$$x = Ax + Bu \tag{12}$$

$$y = Cx \tag{13}$$

In this case the x and y can be substitute using transfer function of plant DC motor in (9).

$$u = u_1 + u_{SF} = ek_1 + Kx \tag{14}$$

$$\dot{e} = r - y = r - Cx \tag{15}$$

$$e = \int \dot{e}\, dt \tag{16}$$

Where the variable x is the state vector of the DC motor plant, e is the output of integrator, $\dot{e}$ is the deviation between the reference and the feedback, u is the control signal, y is the output signal, r is the reference signal, k_1 is the integral parameter constant, K is the state feedback constant, A is the constant matrix, B is the constant matrix, and C is the constant matrix.

2.5. Sliding Mode Controller (SMC)

The SMC offers a robust alternative, particularly in systems with significant nonlinearities or uncertainties [81]. By utilizing a discontinuous control signal to drive system trajectories towards a predefined sliding surface, SMC ensures high precision and resilience against parameter variations

and external disturbances [82]. This controller's robustness is particularly beneficial for DC motors operating under harsh or rapidly changing conditions, where stability and accuracy are critical. SMC's adaptability to nonlinear dynamics makes it a preferred choice for complex control systems requiring rapid response and minimal error [83].

The sliding mode controller needs the model in the state space controllable form. Thus, the transfer function model in (9) can be written in time domain as:

$$\ddot{\omega} + 6.1\dot{\omega} + 1.63\omega = 15v \tag{17}$$

Then, we define the state space variable as:

$$x_1 = \omega \tag{18}$$

$$x_2 = \dot{\omega} \tag{19}$$

$$u = v \tag{20}$$

We, obtain the state-space model in the controllable canonical form as:

$$\dot{x_1} = x2 \tag{21}$$

$$x_2 = -6.1x_2 - 1.63x_1 + 15v \tag{22}$$

The first step to designing the sliding mode controller was designing the sliding mode function as:

$$s = ce + \dot{e} \tag{23}$$

Where the variable e is the tracking error and variable c must satisfy the Hurwitz condition $c > 0$. The tracking error and the derivation are:

$$e = \omega_d - \omega \tag{24}$$

$$\dot{e} = \dot{\omega_d} - \dot{\omega} \tag{25}$$

$$\ddot{e} = \ddot{\omega_d} - \ddot{\omega} \tag{26}$$

Where the variable ω_d is the reference signal, and ω is the actual angular speed. Define the Lyapunov function as:

$$V = \frac{1}{2}s^2 \tag{27}$$

To guarantee the stability condition, the derivation of the Lyapunov function in (28) must be $\dot{V} < 0$ as:

$$s\dot{s} < 0 \tag{28}$$

The derivation of the sliding mode function is:

$$\dot{s} = c\dot{e} + \ddot{e} \tag{29}$$

$$\dot{s} = c\dot{e} + \ddot{\omega_d} - \ddot{\omega} \tag{30}$$

$$\dot{s} = c\dot{e} + \ddot{\omega_d} + 6.1\dot{\omega} + 1.63\omega - 15u \tag{31}$$

Thus, the derivation of the Lyapunov function $\dot{V}$ is:

$$s\dot{s} = s(c\dot{e} + \ddot{\omega}_d + 6.1\dot{\omega} + 1.63\omega - 15u) \tag{32}$$

To satisfy the condition $s\dot{s} < 0$, the sliding mode controller is designed as:

$$u = \frac{1}{15}(1.63\omega + 6.1\dot{\omega} + \ddot{\omega}_d + c\dot{e} + K\ sgn(s)) \tag{33}$$

Where the $sgn(s)$ function value is:

$$sgn(s) = \begin{cases} 1, s > 0 \\ 0, s = 0 \\ -1, s < 0 \end{cases} \tag{34}$$

2.6. Fuzzy Logic Controller (FLC)

Fuzzy Logic is a mathematical approach that handles approximate reasoning, making it suitable for control systems with nonlinear or complex behaviors [84], [85]. A FLC mimics human decision-making by processing imprecise or qualitative information, providing adaptability and robustness [86]. Common types of FLCs include Mamdani [87], Sugeno [88], and Tsukamoto controllers [89].

A Mamdani FLC consists of fuzzification, rule base, inference engine, and defuzzification components [90]. The fuzzification process converts crisp inputs into fuzzy sets using membership functions, such as triangular or Gaussian. The rule base contains expert-defined if-then rules, such as "If the error is large positive and the change in error is small, then the control action should be medium positive" [91]. This research employs Mamdani FLC to achieve adaptive control.

The inference engine processes fuzzy rules and inputs using logical operations like min-max to produce a fuzzy output. The aggregated output is converted into a crisp value via defuzzification methods, such as the centroid or mean of maximum, which is then used to control the system. For instance, the crisp value may regulate a DC motor's speed by adjusting its armature voltage, ensuring precise and adaptive performance.

2.7. Particle Swarm Optimization (PSO)

PSO is a computational method introduced by Russell Eberhart and James Kennedy in 1995, inspired by the social behavior of birds flocking or fish schooling [92]. It is a population-based stochastic optimization technique where a group of potential solutions, called particles [93], navigates through a multidimensional search space to optimize a given objective function like ISE, IAE, ITAE, and ITSE [94]. Each particle adjusts its position and velocity dynamically based on its own best-known position (personal best, pBest) and the best-known position found by the entire swarm (global best, gBest) [95].

The movement of particles in PSO is governed by specific mathematical equations, enabling them to explore the search space efficiently while balancing exploration and exploitation [96]. By combining individual learning with social sharing of information, PSO allows the swarm to converge toward the optimal solution [97]. This flexibility and robustness make PSO a widely used technique for solving various optimization problems across different domains. The procedure of the PSO can be explained in brief as follows:

1. Initialization the swarm with random position and velocities for each particle.
2. Evaluate the fitness of each particle based on the objective function.
3. If the current position of a particle is better that its personal best, update its personal best.
4. If the current position of a particle is better that its global best, update its global best.
5. Update the velocity and position of each particle using the velocity and position update equation.
6. The steps 2-6 should be repeated until a termination criterion is met, such as a maximum number of iterations or a satisfactory fitness value.

3. Results and Discussion

3.1. Simulation Preparation

The simulation for the DC motor control system was conducted on a laptop equipped with an Intel Core i3-1215U processor, 16 GB of RAM, and running Windows 11. The simulation was carried out for 10 seconds, using a time sampling interval of 0.001 seconds to make sure that the data was collected accurately. For optimal controller performance, Particle Swarm Optimization (PSO) was employed to fine-tune the parameters of the PID, FOPID, ISF, and SMC controllers, enhancing their response characteristics and robustness. However, the FLC was implemented without PSO, focusing on its inherent fuzzy logic capabilities to manage the motor's nonlinear dynamics effectively. This setup allowed for a comprehensive comparison of various advanced control techniques under identical simulation conditions.

3.1.1. PID-PSO

In the PID-PSO optimization, the parameters were configured as outlined in the Table 2 to achieve optimal performance. The Simulink model of the DC motor used for this simulation is shown in Fig. 2.

Table 2. PID-PSO parameters configurations

Parameters	Value	Description
numParticles	50	Number of particles in the swarm
numIterations	50	Number of iterations to be performed
c1	1.7	Cognitive parameters (influence of individual speed)
c2	1.4	Social parameters (group speed influence)
w	0.5	Inertia weight (influence of previous speed)
dim	3	Optimised variable dimensions (Kp, Ki, Kd)
Lb	[0.001, 0.001, 0.001]	Lower limit for each variable dimension
Ub	[20, 20, 20]	Upper limit for each variable dimension

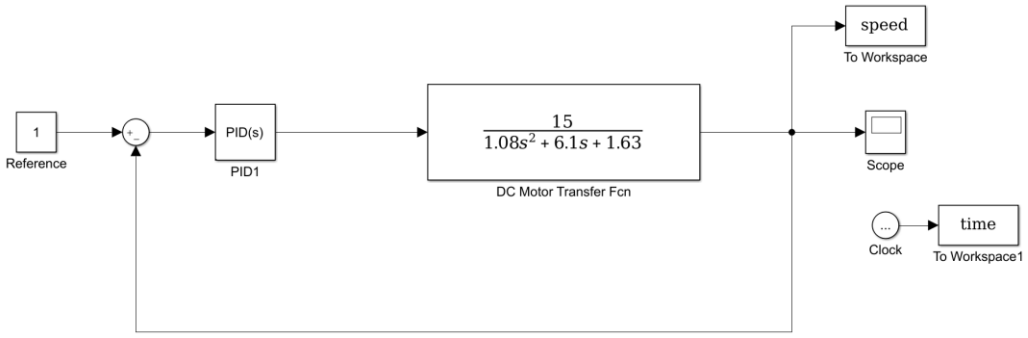

Fig. 2. PID DC Motor simulation model in Simulink

3.1.2. FOPID-PSO

In the FOPID-PSO optimization, the parameters were configured as outlined in the Table 3 to achieve optimal performance. The Simulink model of the DC motor used for this simulation is shown in Fig. 3.

Table 3. FOPID-PSO parameters configurations

Parameters	Value	Description
numParticles	50	Number of particles in the swarm
numIterations	50	Number of iterations to be performed
c1	1.4	Cognitive parameters (influence of individual speed)
c2	1.2	Social parameters (group speed influence)
w	0.4	Inertia weight (influence of previous speed)
dim	5	Optimised variable dimensions (Kp, Ki, Lambda, Kd, Mu)
lb	[0.001, 0.001, 0.001, 0.001, 0.001]	Lower limit for each variable dimension
ub	[20, 20, 1.5, 20, 1.5]	Upper limit for each variable dimension

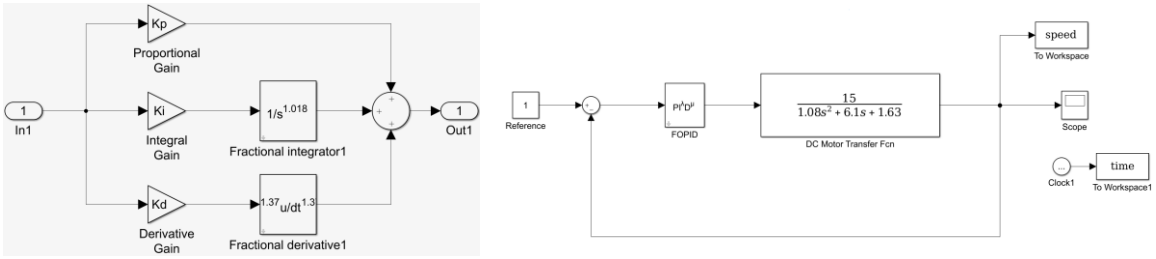

(a) (b)

Fig. 3. FOPID DC motor simulation model in Simulink, (a) FOPID blocks, (b) DC motor using FOPID controllers

3.1.3. ISF-PSO

In the ISF-PSO optimization, the parameters were configured as outlined in the Table 4 to achieve optimal performance. The Simulink model of the DC motor used for this simulation is shown in Fig. 4.

Table 4. ISF-PSO parameters configurations

Parameters	Value	Description
numParticles	50	Number of particles in the swarm
numIterations	50	Number of iterations to be performed
c1	1.6	Cognitive parameters (influence of individual speed)
c2	1.4	Social parameters (group speed influence)
w	0.5	Inertia weight (influence of previous speed)
dim	3	Optimised variable dimensions (Ki, K1, K2)
lb	[0.001, 0.001, 0.001]	Lower limit for each variable dimension
ub	[3000, 500, 50]	Upper limit for each variable dimension

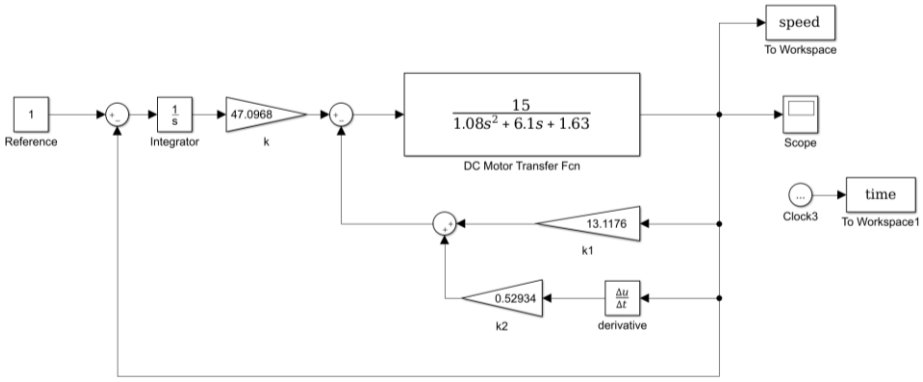

Fig. 4. ISF DC motor simulation model in Simulink

3.1.4. SMC-PSO

In the ISF-PSO optimization, the parameters were configured as outlined in the Table 5 to achieve optimal performance. The Simulink model of the DC motor used for this simulation is shown in Fig. 5.

Table 5. SMC-PSO parameters configurations

Parameters	Value	Description
numParticles	50	Number of particles in the swarm
numIterations	50	Number of iterations to be performed
c1	0.6	Cognitive parameters (influence of individual speed)
c2	0.5	Social parameters (group speed influence)
w	0.1	Inertia weight (influence of previous speed)
dim	3	Optimised variable dimensions (k, k1, k2)
lb	[0.001, 0.001, 0.001]	Lower limit for each variable dimension
ub	[3000, 70, 70]	Upper limit for each variable dimension

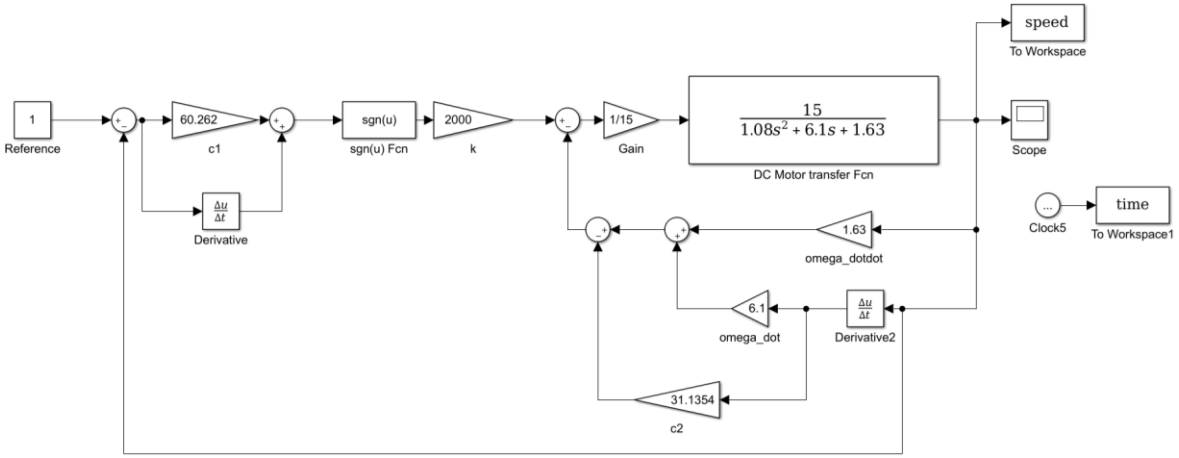

Fig. 5. SMC DC motor simulation model in Simulink

3.1.5. FLC Design

In FLC testing, PSO optimization is not used. The inputs of the FLC controller in this system are used 2, namely error and integral error, with each having three memberships (negative, neutral, and positive), for the output also has 3 memberships (negative, neutral, and positive) in trimf (triangular function). The FLC output has 9 rules which are shown in Table 6. The Simulink model of the DC motor used for this simulation is shown in Fig. 6. FLC DC Motor simulation model in Simulink shown in Fig. 7.

Table 6. FLC output (9 rules)

		Error		
		N	Z	P
Integral Error	N	N	N	Z
	Z	N	Z	P
	P	Z	P	P

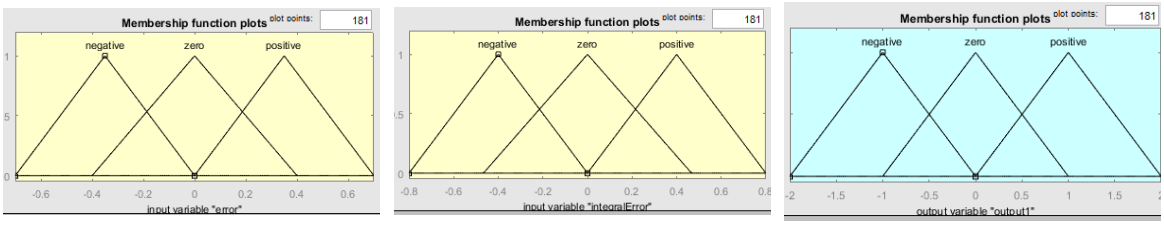

(a) (b) (c)

Fig. 6. Membership function values of FLC input and output variable (a) input 1(error), (b) input 2 (integral error), and (c) output

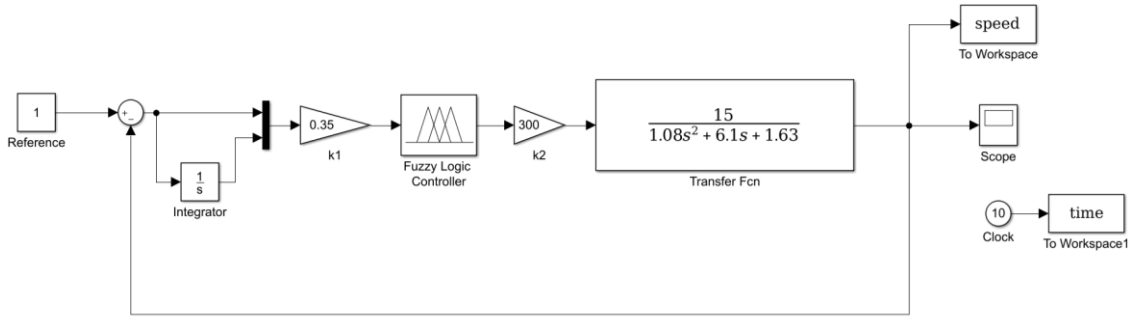

Fig. 7. FLC DC Motor simulation model in Simulink

3.2. Simulation Results

The simulation results in Table 7 showcase the optimal parameters obtained for each controller, highlighting the specific tuning configurations that lead to their best performance. These parameters determined using Particle Swarm Optimization (PSO) for PID, FOPID, ISF, and SMC controllers, include critical variables such as proportional gain, integral gain, derivative gain, and fractional orders for FOPID. For FLC, the rule base and membership functions are presented as the foundation for its control logic, despite being untuned by optimization techniques.

Table 7. Optimal parameter for each controllers

Controllers	Kp	Ki	Kd	Lambda	Mu	K	K1	K2	C1	C2
HBO/HGSO-PID [44]	16.9327	0.9508	2.8512	-	-	-	-	-	-	-
PSO-PID	20.0000	5.7292	6.6310	-	-	-	-	-	-	-
PSO-FOPID	20.0000	18.2389	19.2209	0.6913	0.9850	-	-	-	-	-
OBL-MRFO-SA-FOPID [45]	19.8080	9.9786	9.9504	0.8147	0.9030	-	-	-	-	-
PSO-ISF	-	-	-	-	-	3000	187.7064	2.7085	-	-
PSO-SMC	-	-	-	-	-	2000	-	-	60.2622	31.1354

Based on Fig. 8 and Table 8, the PSO-FOPID controller demonstrates the best overall performance among the compared controllers. It achieves the fastest rise time and settling time, underscoring its ability to respond quickly to changes. This remarkable performance is attributed to the nonlinear characteristics of the fractional integral and derivative components [98], [99], which enhance the controller's ability to adapt to varying system dynamics, despite its overshoot of 0.10794%, the PSO-FOPID controller compensates with the lowest ITSE, indicating superior control accuracy and energy efficiency in managing system errors over time. Same with OBL-MRFO-SA-FOPID [45], but not as better as PSO. These features make it particularly suitable for applications requiring high precision and rapid response. PSO-PID and PSO-SMC also perform well, although they exhibit higher settling times and overshoot compared to PSO-FOPID. OBL/HGSO-PID [44] delivers a response without overshoot but shows lowest stability, as indicated by its larger SSE value compared to the other controllers and slower rise time compared PSO-FOPID, PSO-PID, and PSO-SMC. The PSO-ISF controller, on the other hand, exhibits a high settling time and initial oscillations; however, it stands out with the highest stability, as reflected in its lowest SSE value. This remarkable stability can likely be attributed to the controller's state feedback mechanism [78], [100], which enhances its ability to effectively manage system dynamics. Lastly, the FLC controller shows the worst performance, with an extremely high overshoot (25.2936812%) and a very slow recovery time, making it unsuitable for applications requiring fast response and high precision. Ultimately, the PSO algorithm demonstrates superior performance compared to OBL/HGSO and OBL-MRFO-SA across both PID and FOPID controllers.

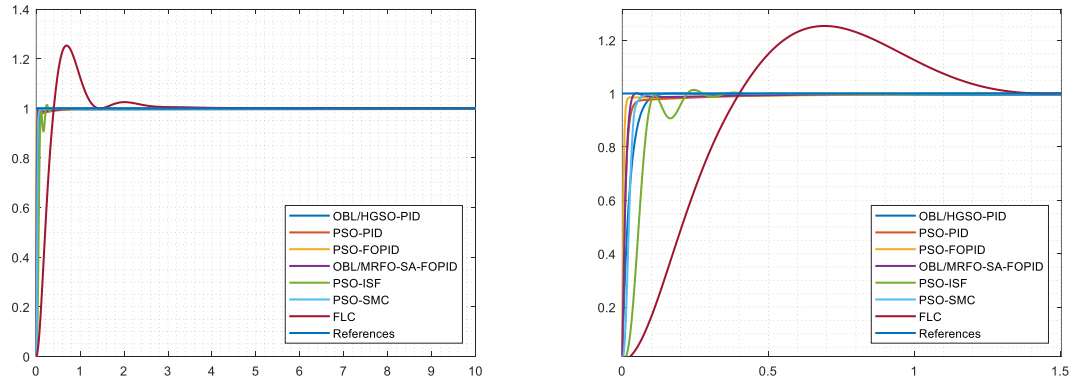

(a) (b)

Fig. 8. Simulation results, (a) 10 seconds, (b) zoomed In

Table 8. Response analysis of each Controllers

Controllers	Rise Time (s)	Settling Time (s)	Overshoot (%)	SSE	ITSE
OBL/HGSO-PID [44]	0.0522738	0.0917148	**0.0000000**	-2.93E-03	0.2003254
PSO-PID	0.0242706	0.1423734	0.0369476	3.73E-05	0.0149693
PSO-FOPID	0.0091033	0.0187095	0.1079422	-3.36E-04	0.0095792
OBL-MRFO-SA-FOPID [45]	0.0211638	0.0331208	0.1107691	-3.00E-04	0.0121425
PSO-ISF	0.0593791	0.2104593	1.3604417	-2.44E-15	0.2982205
PSO-SMC	0.0287702	0.0596133	1.0010182	2.01E-06	0.0473054
FLC	0.2742943	2.2445106	25.2936812	1.99E-06	8.3910457

3.3. Comparison Robustness Analysis

A robust controller is essential to ensure that the system response remains within acceptable limits despite uncertainties and parameter variations. A comprehensive robustness analysis is performed to evaluate the stability and performance of each control system. This analysis involves systematically varying key parameters of the DC motor, specifically the electrical resistance (R_a) and the torque constant (K_m), by ±25% and ±20%, respectively. These variations are designed to simulate real-world conditions where parameters may deviate from their nominal values due to manufacturing tolerances, environmental changes, or wear and tear. The parameter variations result in four distinct operational scenarios, which are detailed in Table 9, allowing for a thorough assessment of the system's robustness and reliability under different conditions.

The comparative simulation results of transient response analysis for all scenarios are shown in Table 10, Table 11, Table 12, Table 13 and Fig. 9 showed the simulation results of robustness variation motor parameter.

Table 9. Variations in Motor Parameters for Robustness Analysis

Motor Parameter	Scenario I	Scenario II	Scenario III	Scenario IV
R_a	0.30	0.30	0.50	0.50
K_m	0.012	0.018	0.012	0.018

Table 10. Scenario I

Controllers	Rise Time (s)	Settling Time (s)	Overshoot (%)	SSE	ITSE
OBL/HGSO-PID [44]	0.0654004	0.1136849	0.0302067	-2.62E-03	0.1890539
PID-PSO	0.0314040	0.2124803	0.1402441	1.24E-04	0.0254702
PSO-FOPID	0.0091033	0.0187095	0.1079422	-3.36E-04	0.0095792
OBL-MRFO-SA-FOPID[45]	0.0261278	0.0424824	0.1502158	-2.29E-04	0.0182151
PSO-ISF	0.0568628	0.3538560	5.6196946	2.22E-15	0.3410601
PSO-SMC	0.0296083	0.0478017	0.1041464	-6.63E-05	0.0571926
FLC	0.3291081	2.3847825	24.2291682	1.65E-06	11.6696925

Table 11. Scenario II

Controllers	Rise Time (s)	Settling Time (s)	Overshoot (%)	SSE	ITSE
OBL/HGSO-PID [44]	0.0433829	0.0756140	0.0824856	-2.32E-03	0.1275648
PID-PSO	0.0195651	0.0699049	0.0404979	3.93E-05	0.0100242
PSO-FOPID	0.0110967	0.0270265	0.1950677	-2.87E-04	0.0143547
OBL-MRFO-SA-FOPID[45]	0.0177165	0.0272167	0.5578180	-2.32E-04	0.0082094
PSO-ISF	0.0637264	0.2014608	0.0621896	2.00E-15	0.2823129
PSO-SMC	0.0323326	0.0674204	0.0824931	-4.88E-04	0.0415854
FLC	0.2354853	2.2913216	28.6577213	2.80E-06	7.4859520

Based on the simulation results for all four scenarios in Table 10, Table 11, Table 12, Table 13 and Fig. 9, the PSO-FOPID controller consistently demonstrates the best overall performance across different system conditions, with the fastest rise time, shortest settling time. Despite minor overshoot, it excels in achieving rapid stabilization. The OBL-MRFO-SA-FOPID perform good, but same not as good with PSO-FOPID. The PSO-PID controller also performs well, with fast response times, although it is less efficient than PSO-FOPID in terms of settling time and ITSE.

Table 12. Scenario III

Controllers	Rise Time (s)	Settling Time (s)	Overshoot (%)	SSE	ITSE
OBL/HGSO-PID [44]	0.0658475	0.1163715	**0.0000000**	-3.86E-03	0.3402864
PID-PSO	0.0315340	0.2357574	0.0323283	3.44E-05	0.0245108
PSO-FOPID	0.0072226	0.0147275	0.0965725	-2.64E-04	0.0063607
OBL-MRFO-SA-FOPID [45]	0.0262024	0.0428143	0.0574448	-4.01E-04	0.0195658
PSO-ISF	0.0569147	0.3536831	5.5929648	2.22E-15	0.3408720
PSO-SMC	0.0297055	0.0480931	0.1015623	-5.30E-04	0.0574814
FLC	0.3356360	1.7085195	22.1025739	1.93E-06	10.6382880

Table 13. Scenario IV

Controllers	Rise Time (s)	Settling Time (s)	Overshoot (%)	SSE	ITSE
OBL/HGSO-PID [44]	0.0435765	0.0768521	0.0000000	-3.14E-03	0.2123940
PID-PSO	0.0196188	0.0816907	0.0000000	-2.06E-05	0.0113335
PSO-FOPID	0.0072257	0.0147922	0.0541756	-3.71E-04	0.0078150
OBL-MRFO-SA-FOPID [45]	0.0177408	0.0273090	0.4942120	-3.47E-04	0.0100917
PSO-ISF	0.0637799	0.2015251	0.0608155	1.33E-15	0.2824289
PSO-SMC	0.0325032	0.0677617	0.0805743	-3.19E-04	0.0417002
FLC	0.2382770	2.2673547	26.9074916	2.89E-06	6.9208616

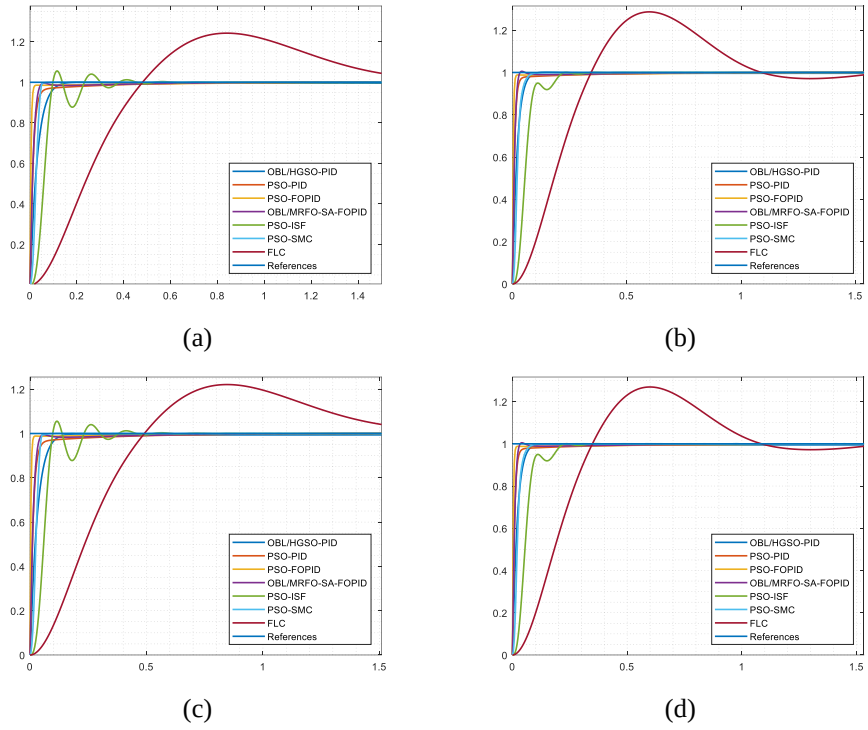

Fig. 9. Simulation Results of Robustness Variation Motor Parameter, (a) Scenario I, (b) Scenario II, (c) Scenario III, and (d) Scenario IV

The OBL/HGSO-PID controller delivers stable performance without overshoot, but its response is slower compared to PSO-PID. The PSO-ISF controller, initially exhibiting high settling times and oscillations, ultimately achieves the highest stability, consistently maintaining the lowest and relatively stable SSE values across all scenarios, which contrasts with its initial behavior and highlights its final performance. The PSO-SMC controller demonstrates good stability but is slightly slower than PSO-ISF, with a higher SSE value. Finally, the FLC controller performs the worst, with the highest overshoot, longest recovery times, and largest ITSE values, making it unsuitable for systems requiring fast and precise control. These results confirm that PSO-FOPID is the most efficient controller overall, with PSO-PID and OBL/HGSO-PID also offering good performance, while PSO-

ISF provides the highest stability and PSO-SMC follows closely behind, regardless of the scenario conditions.

4. Conclusion

The study on DC motor control using various advanced control methods—PID, FOPID, ISF, SMC, and FLC—provides significant insights into their performance and robustness. The primary objective was to compare these controllers' effectiveness in managing speed instability, load variations, and external disturbances, with a focus on optimizing the tuning parameters using PSO for PID, FOPID, ISF, and SMC controllers. The FLC was implemented without PSO to highlight its inherent fuzzy logic capabilities.

The PSO-FOPID controller emerged as the most efficient and reliable option, achieving the fastest rise time of 0.0091 seconds and the shortest settling time of 0.0187 seconds, with the lowest ITSE of 0.0096. Despite a minor overshoot of 0.11%, its ability to handle nonlinear dynamics and external disturbances is commendable, thanks to the flexibility and adaptability of fractional-order terms. The PID-PSO controller also performed well, with a fast rise time of 0.0243 seconds and a low overshoot of 0.037%, though it had a longer settling time of 0.1424 seconds and a higher ITSE of 0.015.

The PSO-SMC controller demonstrated good stability and a reasonable response time, with a settling time of 0.0596 seconds and a slightly higher SSE value of 2.01E-06. It also had a higher ITSE value of 0.047, indicating room for improvement in steady-state accuracy. The PSO-ISF controller stood out for its exceptional stability, consistently maintaining the lowest SSE values, making it ideal for applications requiring high stability, such as in medical devices or safety-critical systems. The OBL/HGSO-PID controller, while stable and overshoot-free, had a slower response time of 0.0917 seconds and a higher SSE of -2.93E-03, placing it behind the PSO- SMC and PSO-ISF controllers in overall performance.

The FLC controller performed the worst, with the highest overshoot of 25.2936812% and the longest recovery times, with a settling time of 2.2445 seconds. The high ITSE value of 8.391 further underscores its limitations in maintaining accurate and stable performance. The robustness analysis further reinforces the superiority of the PSO-FOPID controller, which outperforms OBL/HGSO and OBL-MRFO-SA optimizations across both PID and FOPID controllers. These findings underscore the PSO-FOPID controller's reliability and adaptability, making it the preferred choice for DC motor control in demanding environments requiring precision, stability, and robustness.

Author Contribution: All authors contributed equally to the main contributor to this paper. All authors read and approved the final paper.

Funding: This research received funding from Universitas Ahmad Dahlan grant research.

Conflicts of Interest: The authors declare no conflict of interest.

References

[1] A. H. Sabry, A. H. Shallal, H. S. Hameed, and P. J. Ker, “Compatibility of household appliances with DC microgrid for PV systems,” *Heliyon*, vol. 6, no. 12, p. e05699, 2020, https://doi.org/10.1016/j.heliyon.2020.e05699.

[2] M. Nandakumar, S. Ramalingam, S. Nallusamy, and S. Srinivasarangan Rangarajan, “Hall-Sensor-Based Position Detection for Quick Reversal of Speed Control in a BLDC Motor Drive System for Industrial Applications,” *Electronics*, vol. 9, no. 7, p. 1149, 2020, https://doi.org/10.3390/electronics9071149.

[3] N. Shah, W.Y. Park, and C. Ding, “Trends in best-in-class energy-efficient technologies for room air conditioners,” *Energy Reports*, vol. 7, pp. 3162-3170, 2021, https://doi.org/10.1016/j.egyr.2021.05.016.

[4] D. Mohanraj *et al*., "A Review of BLDC Motor: State of Art, Advanced Control Techniques, and Applications," *IEEE Access*, vol. 10, pp. 54833-54869, 2022, https://doi.org/10.1109/ACCESS.2022.3175011.

[5] K. Mohammed, J. A. F. Yahaya, and R. B. Khan, "Applied measurement of the motor speed controller for washing machine with random loads, part II," *International Journal of Power Electronics and Drive Systems (IJPEDS)*, vol. 11, no. 1, pp. 442-450, 2020, http://doi.org/10.11591/ijpeds.v11.i1.pp442-450.

[6] Y. Choo *et al*., "Investigation of Systematic Efficiency in a High-Speed Single-Phase Brushless DC Motor Using Multi-Physics Analysis for a Vacuum Cleaner," *IEEE Transactions on Magnetics*, vol. 55, no. 7, pp. 1-6, 2019, https://doi.org/10.1109/TMAG.2019.2903445.

[7] V. S. Panwar, A. Pandey, and M. E. Hasan, "Design and fabrication of a novel concept-based autonomous controlled solar powered four-wheeled Floor Cleaning Robot for wet and dry surfaces," *International Journal of Information Technology*, vol. 14, no. 4, pp. 1995-2004, 2022, https://doi.org/10.1007/s41870-022-00893-1.

[8] O. V. Shepovalova, A. T. Belenov, and S. V. Chirkov, "Review of photovoltaic water pumping system research," *Energy Reports*, vol. 6, pp. 306-324, 2020, https://doi.org/10.1016/j.egyr.2020.08.053.

[9] H. Yang, Z. Wang, T. Zhang, and F. Du, "A review on vibration analysis and control of machine tool feed drive systems," *The International Journal of Advanced Manufacturing Technology*, vol. 107, pp. 503-525, 2020, https://doi.org/10.1007/s00170-020-05041-2.

[10] Y. M. Hendrawan, A. Farrage, and N. Uchiyama, "Iterative NC program modification and energy saving for a CNC machine tool feed drive system with linear motors," *The International Journal of Advanced Manufacturing Technology*, vol. 102, pp. 3543-3562, 2019, https://doi.org/10.1007/s00170-019-03390-1.

[11] A. Ramaswamy and M. Muniraj, "Investigation of an Intellectual Tracking System Using the Intelligent Controller for Infusion Pump in Medical Applications," *Brazilian Archives of Biology and Technology*, vol. 67, 2024, https://doi.org/10.1007/s00170-019-03390-1.

[12] L. A. O'Connor, B. Houseman, T. Cook, and C. C. Quinn, "Intercostal cryonerve block versus elastomeric infusion pump for postoperative analgesia following surgical stabilization of traumatic rib fractures," *Injury*, vol. 54, no. 11, p. 111053, 2023, https://doi.org/10.1007/s00170-019-03390-1.

[13] V. Sankardoss and P. Geethanjali, "Design and Low-Cost Implementation of an Electric Wheelchair Control," *IETE Journal of Research*, vol. 67, no. 5, pp. 657–666, 2021, https://doi.org/10.1080/03772063.2019.1565951.

[14] J. Arcos-Legarda and A. Tovar, "Mechatronic Design and Active Disturbance Rejection Control of a Bag Valve-Based Mechanical Ventilator," *Journal of Medical Devices*, vol. 15, no. 3, p. 031006, 2021, https://doi.org/10.1115/1.4051064.

[15] R. Hernandez-Alvarado, O. Rodriguez-Abreo, J. M. Garcia-Guendulain, and T. Hernandez-Diaz, "Self-Tuning Control Using an Online-Trained Neural Network to Position a Linear Actuator," *Micromachines*, vol. 13, no. 5, p. 696, 2022, https://doi.org/10.3390/mi13050696.

[16] R. Saputra, and N. Surantha, "Smart and real-time door lock system for an elderly user based on face recognition," *Bulletin of Electrical Engineering and Informatics*, vol. 10, no. 3, pp. 1345-1355, 2021, https://doi.org/10.11591/eei.v10i3.2955.

[17] J. Guntur, S. S. Raju, T. Niranjan, S. K. Kilaru, R. Dronavalli, and N. S. S. Kumar, "IoT-Enhanced Smart Door Locking System with Security," *SN Computer Science*, vol. 4, no. 2, p. 209, 2023, https://doi.org/10.1007/s42979-022-01641-9.

[18] F. Z. Baouche *et al*., "Design and Simulation of a Solar Tracking System for PV," *Applied Sciences*, vol. 12, no. 19, p. 9682, 2022, https://doi.org/10.3390/app12199682.

[19] A. Karabiber and Y. Güneş, "Single-motor and dual-axis solar tracking system for micro photovoltaic power plants," *Journal of Solar Energy Engineering*, vol. 145, no. 5, p.051004, 2023, https://doi.org/10.1115/1.4056739.

[20] S. S. Nielsen, R. K. Holm and P. O. Rasmussen, "Conveyor System With a Highly Integrated Permanent Magnet Gear and Motor," *IEEE Transactions on Industry Applications*, vol. 56, no. 3, pp. 2550-2559, 2020, https://doi.org/10.1109/TIA.2020.2977877.

[21] M. Q. Zaman and H. -M. Wu, "Intelligent Motion Control Design for an Omnidirectional Conveyor System," *IEEE Access*, vol. 11, pp. 47351-47361, 2023, https://doi.org/10.1109/ACCESS.2023.3275962.

[22] S. Sukamta, A. Nugroho, Subiyanto, R. Rezianto, M. F. Soambaton, and A. Ardiyanto, "Image-Based Position Control for Three-Wheel Omni-Directional Robot," *Jurnal Ilmiah Teknik Elektro Komputer dan Informatika (JITEKI)*, vol. 10, no. 3, pp. 566-579, 2024, https://doi.org/10.26555/jiteki.v10i3.29601.

[23] S. H. Yen, P. C. Tang, Y. C. Lin, and C. Y. Lin, "A sensorless and low-gain brushless DC motor controller using a simplified dynamic force compensator for robot arm application," *Sensors*, vol. 19, no. 14, p. 3171, 2019, https://doi.org/10.3390/s19143171.

[24] Fahmizal, M. S. Pratikno, H. N. Isnianto, A. Mayub, H. Maghfiroh, and P. Anugrah, "Control and Navigation of Differential Drive Mobile Robot with PID and Hector SLAM: Simulation and Implementation," *Jurnal Ilmiah Teknik Elektro Komputer dan Informatika (JITEKI)*, vol. 10, no. 3, pp. 594–607, 2024, https://doi.org/10.26555/jiteki.v10i3.29428.

[25] N. X. Chiem, "Cascade Control for Trajectory-Tracking Mobile Robots Based on Synergetic Control Theory and Lyapunov Functions," *Control Systems and Optimization Letters*, vol. 3, no. 1, pp. 14-19, 2025, https://doi.org/10.59247/csol.v3i1.169.

[26] H. Khan, S. Khatoon, and P. Gaur, "Comparison of various controller design for the speed control of DC motors used in two wheeled mobile robots," *International Journal of Information Technology*, vol. 13, no. 2, pp. 713-720, 2021, https://doi.org/10.1007/s41870-020-00577-8.

[27] C. Iwendi, M. A. Alqarni, J. H. Anajemba, A. S. Alfakeeh, Z. Zhang and A. K. Bashir, "Robust Navigational Control of a Two-Wheeled Self-Balancing Robot in a Sensed Environment," *IEEE Access*, vol. 7, pp. 82337-82348, 2019, https://doi.org/10.1109/ACCESS.2019.2923916.

[28] G. Curiel-Olivares, J. Linares-Flores, J. F. Guerrero-Castellanos, and A. Hernández-Méndez, "Self-balancing based on Active Disturbance Rejection Controller for the Two-In-Wheeled Electric Vehicle, Experimental results," *Mechatronics*, vol. 76, p. 102552, 2021, https://doi.org/10.1016/j.mechatronics.2021.102552.

[29] Y. Yaşa, "An Efficient Brushless DC Motor Design for Unmanned Aerial Vehicles," *European Journal of Science and Technology*, no. 35, pp. 288-294, 2022, https://doi.org/10.31590/ejosat.1083838.

[30] A. Bosso, C. Conficoni, D. Raggini and A. Tilli, "A Computational-Effective Field-Oriented Control Strategy for Accurate and Efficient Electric Propulsion of Unmanned Aerial Vehicles," *IEEE/ASME Transactions on Mechatronics*, vol. 26, no. 3, pp. 1501-1511, 2021, https://doi.org/10.1109/TMECH.2020.3022379.

[31] Y. Jouili, R. Garraoui, M. Ben Hamed, and L. Sbita, "Self-Adaptive PI-FLC for BLDC Motor Speed Supplied by PEM Fuel Cell Stack Optimized by MPPT," *Arabian Journal for Science and Engineering*, vol. 49, no. 5, pp. 6487–6503, 2024, https://doi.org/10.1007/s13369-023-08265-y.

[32] B. Darmono, H. Pranoto, and Z. Arifin, "Torque Analysis of 2 KW BLDC (Brushless Direct Current) Motor with Speed Variations in Electric Cars E-Falco," *International Journal of Advanced Technology in Mechanical, Mechatronics and Materials*, vol. 2, no. 2, pp. 76–86, 2021, https://doi.org/10.37869/ijatec.v2i2.47.

[33] F. A. Pamuji *et al*., "Application of Artificial Neural Network for Speed Control of BLDC Motor 90KW in Electrical Bus," *Przegląd Elektrotechniczny*, vol. 1, no. 2, pp. 205–212, 2022, https://doi.org/10.15199/48.2022.02.47.

[34] T. K. Nizami, A. Chakravarty, C. Mahanta, A. Iqbal, and A. Hosseinpour, "Enhanced dynamic performance in DC–DC converter-PMDC motor combination through an intelligent non-linear adaptive control scheme," *IET Power Electronics*, vol. 15, no. 15, pp. 1607–1616, 2022, https://doi.org/10.15199/48.2022.02.47.

[35] S. Ekinci, D. Izci and M. Yilmaz, "Efficient Speed Control for DC Motors Using Novel Gazelle Simplex Optimizer," *IEEE Access*, vol. 11, pp. 105830-105842, 2023, https://doi.org/10.1109/ACCESS.2023.3319596.

[36] F. Alanazi, "Electric Vehicles: Benefits, Challenges, and Potential Solutions for Widespread Adaptation," *Applied Sciences*, vol. 13, no. 10, p. 6016, 2023, https://doi.org/10.3390/app13106016.

[37] X. Zhu, H. Shi, C. Zhang, Y. Du, L. Xu and L. Zhang, "Speed Ripple Suppression of Permanent Magnet Hub Motor Based on ADRC With Observer Error Constraints," *IEEE Transactions on Industrial Electronics*, vol. 72, no. 2, pp. 1205-1216, 2025, https://doi.org/10.1109/TIE.2024.3409902.

[38] Q. Xu, Y. Wang, X. Chen, and W. Cao, "Research on Dynamic Reactive Power Cost Optimization in Power Systems with DFIG Wind Farms," *Processes*, vol. 12, no. 5, p. 872, 2024, https://doi.org/10.3390/pr12050872.

[39] H. Djouadi, K. Ouari, Y. Belkhier, H. Lehouche, M. Bajaj, and V. Blazek, "Improved robust model predictive control for PMSM using backstepping control and incorporating integral action with experimental validation," *Results in Engineering*, vol. 23, p. 102416, 2024, https://doi.org/10.1016/j.rineng.2024.102416.

[40] J. Rodriguez *et al*., "Latest Advances of Model Predictive Control in Electrical Drives—Part I: Basic Concepts and Advanced Strategies," *IEEE Transactions on Power Electronics*, vol. 37, no. 4, pp. 3927-3942, 2022, https://doi.org/10.1109/TPEL.2021.3121532.

[41] K. Xu, W. Liang, W. Zhao, C. Wang, S. Zou and X. Zhou, "Vehicle Stability and Synchronization Control of Dual-Motor Steer-by-Wire System Considering Multiple Uncertainties," *IEEE Transactions on Transportation Electrification*, vol. 10, no. 2, pp. 3092-3104, 2024, https://doi.org/10.1109/TTE.2023.3304048.

[42] A. Lotfy, M. Kaveh, M. R. Mosavi, and A. R. Rahmati, "An enhanced fuzzy controller based on improved genetic algorithm for speed control of DC motors," *Analog Integr Circuits Signal Process*, vol. 105, no. 2, pp. 141–155, 2020, https://doi.org/10.1007/s10470-020-01599-9.

[43] A. Irawan, M. H. Sulaiman, M. S. Ramli, and M. I. P. Azahar, "Pneumatic servo position control optimization using adaptive-domain prescribed performance control with evolutionary mating algorithm," *Results in Control and Optimization*, vol. 15, p. 100434, 2024, https://doi.org/10.1016/j.rico.2024.100434.

[44] S. Ekinci, B. Hekimoğlu, and D. Izci, "Opposition based Henry gas solubility optimization as a novel algorithm for PID control of DC motor," *Engineering Science and Technology, an International Journal*, vol. 24, no. 2, pp. 331–342, 2021, https://doi.org/10.1016/j.jestch.2020.08.011.

[45] S. Ekinci, D. Izci, and B. Hekimoğlu, "Optimal FOPID Speed Control of DC Motor via Opposition-Based Hybrid Manta Ray Foraging Optimization and Simulated Annealing Algorithm," *Arabian Journal for Science and Engineering*, vol. 46, no. 2, pp. 1395–1409, 2021, https://doi.org/10.1007/s13369-020-05050-z.

[46] B. Zhang and X. Tang, "High-performance state feedback controller for permanent magnet synchronous motor," *ISA Transactions*, vol. 118, pp. 144–158, 2021, https://doi.org/10.1016/j.isatra.2021.02.009.

[47] M. Zhang, X. Jing, W. Huang, and P. Li, "Saturated PD-SMC method for suspension systems by exploiting beneficial nonlinearities for improved vibration reduction and energy-saving performance," *Mechanical Systems and Signal Processing*, vol. 179, p. 109376, 2022, https://doi.org/10.1016/j.ymssp.2022.109376.

[48] X. He *et al*., "Improved beluga whale optimization-based variable universe fuzzy controller for brushless direct current motors of electric tractors," *Computers and Electrical Engineering*, vol. 120, p. 109866, 2024, https://doi.org/10.1016/j.compeleceng.2024.109866.

[49] B. F. Barreiros, J. O. Trierweiler, and M. Farenzena, "Reliable and straightforward PID tuning rules for highly underdamped systems," *Brazilian Journal of Chemical Engineering*, vol. 38, no. 4, pp. 731–745, 2021, https://doi.org/10.1016/j.compeleceng.2024.109866.

[50] D. Gupta, V. Goyal, and J. Kumar, "Comparative performance analysis of fractional-order nonlinear PID controller for complex surge tank system: tuning through machine learning control approach," *Multimedia Tools and Applications*, vol. 83, no. 33, pp. 78923–78956, 2024, https://doi.org/10.1007/s11042-024-18427-1.

[51] Y. Liu *et al*., "Dynamic State Estimation for Power System Control and Protection," *IEEE Transactions on Power Systems*, vol. 36, no. 6, pp. 5909-5921, 2021, https://doi.org/10.1109/TPWRS.2021.3079395.

[52] W. Qi, G. Zong, Y. Hou and M. Chadli, "SMC for Discrete-Time Nonlinear Semi-Markovian Switching Systems With Partly Unknown Semi-Markov Kernel," *IEEE Transactions on Automatic Control*, vol. 68, no. 3, pp. 1855-1861, 2023, https://doi.org/10.1109/TAC.2022.3169584.

[53] K. Sivakumar and S. Appasamy, "Fuzzy Mathematical Approach for Solving Multi-Objective Fuzzy Linear Fractional Programming Problem with Trapezoidal Fuzzy Numbers," *Mathematical Modelling of Engineering Problems*, vol. 11, no. 1, pp. 255–262, 2024, https://doi.org/10.18280/mmep.110128.

[54] R. Szczepanski, M. Kaminski, and T. Tarczewski, "Auto-Tuning Process of State Feedback Speed Controller Applied for Two-Mass System," *Energies*, vol. 13, no. 12, p. 3067, 2020, https://doi.org/10.3390/en13123067.

[55] B. N. Kommula and V. R. Kota, "Design of MFA-PSO based fractional order PID controller for effective torque controlled BLDC motor," *Sustainable Energy Technologies and Assessments*, vol. 49, p. 101644, 2022, https://doi.org/10.1016/j.seta.2021.101644.

[56] M. G. M. Abdolrasol, M. A. Hannan, S. M. S. Hussain, and T. S. Ustun, "Optimal PI controller based PSO optimization for PV inverter using SPWM techniques," *Energy Reports*, vol. 8, pp. 1003–1011, 2022, https://doi.org/10.1016/j.egyr.2021.11.180.

[57] H. Abdelfattah, A. O. Aseeri, and M. Abd Elaziz, "Optimized FOPID controller for nuclear research reactor using enhanced planet optimization algorithm," *Alexandria Engineering Journal*, vol. 97, pp. 267–282, 2024, https://doi.org/10.1016/j.aej.2024.04.021.

[58] S. K. Majhi, M. Sahoo, and R. Pradhan, "Oppositional Crow Search Algorithm with mutation operator for global optimization and application in designing FOPID controller," *Evolving Systems*, vol. 12, no. 2, pp. 463–488, 2021, https://doi.org/10.1007/s12530-019-09305-5.

[59] S. Arun and T. Manigandan, "Design of ACO based PID controller for zeta converter using reduced order methodology," *Microprocessors and Microsystems*, vol. 81, p. 103629, 2021, https://doi.org/10.1016/j.micpro.2020.103629.

[60] B. Arun, B. V. Manikandan, and K. Premkumar, "Multiarea Power System Performance Measurement using Optimized PID Controller," *Microprocessors and Microsystems*, p. 104238, 2021, https://doi.org/10.1016/j.micpro.2021.104238.

[61] M. N. Ali, M. Soliman, K. Mahmoud, J. M. Guerrero, M. Lehtonen and M. M. F. Darwish, "Resilient Design of Robust Multi-Objectives PID Controllers for Automatic Voltage Regulators: D-Decomposition Approach," *IEEE Access*, vol. 9, pp. 106589-106605, 2021, https://doi.org/10.1109/ACCESS.2021.3100415.

[62] M. Khamies, G. Magdy, M. Ebeed, and S. Kamel, "A robust PID controller based on linear quadratic gaussian approach for improving frequency stability of power systems considering renewables," *ISA Transactions*, vol. 117, pp. 118–138, 2021, https://doi.org/10.1016/j.isatra.2021.01.052.

[63] F. Naz *et al*., "PID Tuning with reference tracking and plant uncertainty along with disturbance rejection," *Systems Science & Control Engineering*, vol. 9, no. 1, pp. 160–166, 2021, https://doi.org/10.1080/21642583.2021.1888817.

[64] L. Hazeleger, R. Beerens and N. van de Wouw, "Proportional–Integral–Derivative-Based Learning Control for High-Accuracy Repetitive Positioning of Frictional Motion Systems," *IEEE Transactions on Control Systems Technology*, vol. 29, no. 4, pp. 1652-1663, 2021, https://doi.org/10.1109/TCST.2020.3017803.

[65] P. Razmi, T. Rahimi, K. Sabahi, M. Gheisarnejad, and M. Khooban, "Adaptive fuzzy gain scheduling PID controller for frequency regulation in modern power system," *IET Renewable Power Generation*, vol. 2022, no. 1, pp. 1-16, 2022, https://doi.org/10.1049/rpg2.12569.

[66] L. Wang, J. Liu, C. Yang, and D. Wu, "A novel interval dynamic reliability computation approach for the risk evaluation of vibration active control systems based on PID controllers," *Applied Mathematical Modelling*, vol. 92, pp. 422–446, 2021, https://doi.org/10.1016/j.apm.2020.11.007.

[67] M. Sharma, S. Sharma, and J. Vajpai, "A novel approach to design and analyze fractional order PID controller for speed control of brushless DC motor," *Renewable Energy and Sustainable Development*, vol. 10, no. 2, p. 279, 2024, http://dx.doi.org/10.21622/resd.2024.10.2.903.

[68] M. Huba, S. Chamraz, P. Bistak, and D. Vrancic, “Making the PI and PID Controller Tuning Inspired by Ziegler and Nichols Precise and Reliable,” *Sensors*, vol. 21, no. 18, p. 6157, 2021, https://doi.org/10.3390/s21186157.

[69] D. A. Souza, J. G. Batista, L. L. N. dos Reis, and A. B. S. Júnior, “PID controller with novel PSO applied to a joint of a robotic manipulator,” *Journal of the Brazilian Society of Mechanical Sciences and Engineering*, vol. 43, no. 8, p. 377, 2021, https://doi.org/10.1007/s40430-021-03092-4.

[70] A. Ali, K. Bingi, R. Ibrahim, P. A. M. Devan, and K. B. Devika, “A review on FPGA implementation of fractional-order systems and PID controllers,” *AEU-International Journal of Electronics and Communications*, vol. 177, p. 155218, 2024, https://doi.org/10.1016/j.aeue.2024.155218.

[71] E. A. Mohamed, E. M. Ahmed, A. Elmelegi, M. Aly, O. Elbaksawi and A. -A. A. Mohamed, "An Optimized Hybrid Fractional Order Controller for Frequency Regulation in Multi-Area Power Systems," *IEEE Access*, vol. 8, pp. 213899-213915, 2020, https://doi.org/10.1109/ACCESS.2020.3040620.

[72] B. Khokhar, S. Dahiya, and K. P. S. Parmar, “A novel fractional order proportional integral derivative plus second-order derivative controller for load frequency control,” *International Journal of Sustainable Energy*, vol. 40, no. 3, pp. 235–252, 2021, https://doi.org/10.1080/14786451.2020.1803861.

[73] W. Zheng, Y. Chen, X. Wang, M. Lin, and J. Guo, “Robust fractional order PID controller synthesis for the first order plus integral system,” *Measurement and Control*, vol. 56, no. 1–2, pp. 202–214, 2023, https://doi.org/10.1177/00202940221095564.

[74] O. W. Abdulwahhab, “Design of a Complex fractional Order PID controller for a First Order Plus Time Delay system,” *ISA Transactions*, vol. 99, pp. 154–158, 2020, https://doi.org/10.1016/j.isatra.2019.10.010.

[75] R. Mok and M. A. Ahmad, “Fast and optimal tuning of fractional order PID controller for AVR system based on memorizable-smoothed functional algorithm,” *Engineering Science and Technology, an International Journal*, vol. 35, p. 101264, 2022, https://doi.org/10.1016/j.jestch.2022.101264.

[76] M. A. Ebrahim, M. Becherif, and A. Y. Abdelaziz, “PID-/FOPID-based frequency control of zero-carbon multisources-based interconnected power systems underderegulated scenarios,” *International Transactions on Electrical Energy Systems*, vol. 31, no. 2, 2021, https://doi.org/10.1002/2050-7038.12712.

[77] A. Rajendran, M. Karthikeyan, and G. Saravanakumar, “Implementation of FOPID controller with modified harmony search optimization for precise modelling and auto-tuning of nonlinear systems,” *Automatika*, vol. 65, no. 3, pp. 881-893, 2024, https://doi.org/10.1080/00051144.2024.2307227.

[78] I. Iswanto and A. Ma’arif, "Robust Integral State Feedback Using Coefficient Diagram in Magnetic Levitation System," *IEEE Access*, vol. 8, pp. 57003-57011, 2020, https://doi.org/10.1109/ACCESS.2020.2981840.

[79] H. Du, J. Shi, J. Chen, Z. Zhang, and X. Feng, “High-gain observer-based integral sliding mode tracking control for heavy vehicle electro-hydraulic servo steering systems,” *Mechatronics*, vol. 74, p. 102484, 2021, https://doi.org/10.1016/j.mechatronics.2021.102484.

[80] A. Ma’arif, I. Suwarno, E. Nur’aini, and N. M. Raharja, “Altitude Control of UAV Quadrotor Using PID and Integral State Feedback,” *BIO Web Conferences*, vol. 65, p. 07011, 2023, https://doi.org/10.1051/bioconf/20236507011.

[81] B. Lu, Y. Fang and N. Sun, "Continuous Sliding Mode Control Strategy for a Class of Nonlinear Underactuated Systems," *IEEE Transactions on Automatic Control*, vol. 63, no. 10, pp. 3471-3478, 2018, https://doi.org/10.1109/TAC.2018.2794885.

[82] X. Yu, Y. Feng and Z. Man, "Terminal Sliding Mode Control – An Overview," *IEEE Open Journal of the Industrial Electronics Society*, vol. 2, pp. 36-52, 2021, https://doi.org/10.1109/OJIES.2020.3040412.

[83] S. M. Amrr and A. Alturki, "Robust Control Design for an Active Magnetic Bearing System Using Advanced Adaptive SMC Technique," *IEEE Access*, vol. 9, pp. 155662-155672, 2021, https://doi.org/10.1109/ACCESS.2021.3129140.

[84] H. H. Tang and N. S. Ahmad, "Fuzzy logic approach for controlling uncertain and nonlinear systems: a comprehensive review of applications and advances," *Systems Science & Control Engineering*, vol. 12, no. 1, 2024, https://doi.org/10.1080/21642583.2024.2394429.

[85] F. Sabahi, "Optimal bounded policy for nonlinear tracking control of unknown constrained-input systems," *Transactions of the Institute of Measurement and Control*, vol. 47, no. 3, pp. 585-598, 2024, https://doi.org/10.1177/01423312241254590.

[86] J. Zhao, T. Zhao, K. Nie, and Y. Mao, "A Fuzzy Dual Closed-Loop Control Scheme for Precision Stabilized Platform," *International Journal of Fuzzy Systems*, 2024, https://doi.org/10.1007/s40815-024-01882-1.

[87] M. Praharaj, D. Sain, and B. M. Mohan, "Development, experimental validation, and comparison of interval type-2 Mamdani fuzzy PID controllers with different footprints of uncertainty," *Information Sciences*, vol. 601, pp. 374–402, 2022, https://doi.org/10.1016/j.ins.2022.03.095.

[88] R. Datta, R. Saravanakumar, R. Dey, B. Bhattacharya, and C. K. Ahn, "Improved stabilization criteria for Takagi–Sugeno fuzzy systems with variable delays," *Information Sciences*, vol. 579, pp. 591–606, 2021, https://doi.org/10.1016/j.ins.2021.07.089.

[89] H. Yonezawa, A. Yonezawa, T. Hatano, S. Hiramatsu, C. Nishidome, and I. Kajiwara, "Fuzzy-reasoning-based robust vibration controller for drivetrain mechanism with various control input updating timings," *Mechanism and Machine Theory*, vol. 175, p. 104957, 2022, https://doi.org/10.1016/j.mechmachtheory.2022.104957.

[90] Q. A. Tarbosh *et al*., "Review and Investigation of Simplified Rules Fuzzy Logic Speed Controller of High Performance Induction Motor Drives," *IEEE Access*, vol. 8, pp. 49377-49394, 2020, https://doi.org/10.1109/ACCESS.2020.2977115.

[91] D. Kalibatiene and J. Miliauskaitė, "A dynamic fuzzification approach for interval type-2 membership function development: case study for QoS planning," *Soft computing*, vol. 25, no. 16, pp. 11269–11287, 2021, https://doi.org/10.1007/s00500-021-05899-8.

[92] Ş. Yıldırım, M. S. Bingol, and S. Savas, "Tuning PID controller parameters of the DC motor with PSO algorithm," *International Review of Applied Sciences and Engineering*, vol. 15, no. 3, pp. 281–286, 2024, https://doi.org/10.1556/1848.2023.00698.

[93] D. Zhang, G. Ma, Z. Deng, Q. Wang, G. Zhang, and W. Zhou, "A self-adaptive gradient-based particle swarm optimization algorithm with dynamic population topology," *Applied Soft Computing*, vol. 130, p. 109660, 2022, https://doi.org/10.1016/j.asoc.2022.109660.

[94] S. M. H. Mousakazemi, "Comparison of the error-integral performance indexes in a GA-tuned PID controlling system of a PWR-type nuclear reactor point-kinetics model," *Progress in Nuclear Energy*, vol. 132, p. 103604, 2021, https://doi.org/10.1016/j.pnucene.2020.103604.

[95] O. M. A. Al-hotmani, M. A. Al-Obaidi, J.-P. Li, Y. M. John, R. Patel, and I. M. Mujtaba, "A multi-objective optimisation framework for MED-TVC seawater desalination process based on particle swarm optimisation," *Desalination*, vol. 525, p. 115504, 2022, https://doi.org/10.1016/j.desal.2021.115504.

[96] R. K. Agrawal, B. Kaur, and P. Agarwal, "Quantum inspired Particle Swarm Optimization with guided exploration for function optimization," *Applied Soft Computing*, vol. 102, p. 107122, 2021, https://doi.org/10.1016/j.asoc.2021.107122.

[97] B. Zhao *et al*., "PriMPSO: A Privacy-Preserving Multiagent Particle Swarm Optimization Algorithm," *IEEE Transactions on Cybernetics*, vol. 53, no. 11, pp. 7136-7149, 2023, https://doi.org/10.1109/TCYB.2022.3224169.

[98] P. Chen and Y. Luo, "Analytical Fractional-Order PID Controller Design With Bode's Ideal Cutoff Filter for PMSM Speed Servo System," *IEEE Transactions on Industrial Electronics*, vol. 70, no. 2, pp. 1783-1793, 2023, https://doi.org/10.1109/TIE.2022.3158009.

[99] Y. Wang, M. Pan, W. Zhou, and J. Huang, "Direct thrust control for variable cycle engine based on fractional order PID-nonlinear model predictive control under off-nominal operation conditions," *Aerospace Science and Technology*, vol. 143, p. 108726, 2023, https://doi.org/10.1016/j.ast.2023.108726.

[100] J. Huang, Z. Lv, and J.-Q. Sun, "Optimal full-state feedback observer integrated backstepping control of chemical processes with unknown internal dynamics," *ISA Transactions*, vol. 122, pp. 371–379, 2022, https://doi.org/10.1016/j.isatra.2021.05.009.